

# Dynamics of the Subthalamo-pallidal Complex in Parkinson's Disease During Deep Brain Stimulation

J. Modolo · J. Henry · A. Beuter

Received: 19 April 2008 / Accepted: 16 June 2008 /  
Published online: 1 August 2008  
© Springer Science + Business Media B.V. 2008

**Abstract** The dynamics of the subthalamo-pallidal complex in Parkinson's disease during deep brain stimulation (DBS) were studied using two models, a simple firing-rate model and a population-based model. We extended the simple firing-rate model of the complex formed by the subthalamic nucleus (STN) and the external segment of the Globus Pallidus (GPe) to explore its dynamical regime during DBS. More specifically, the modulation of neuronal activity (i.e., pattern and amplitude) during DBS was studied. A similar approach was used with the population-based model. Simulation results revealed a gradual decrease in bursting activity in STN cells when the DBS frequency increased. In addition, the contribution of the stimulation current type (mono- or biphasic) to the results was also examined. A comparison of the two models indicated that the population-based model was more biologically realistic and more appropriate for exploring DBS mechanisms. Understanding the underlying mechanisms of DBS is a prerequisite for developing new stimulation protocols.

**Keywords** Deep brain stimulation · Subthalamo-pallidal complex · Population dynamics · Firing-rate models

## 1 Introduction

The use of deep brain stimulation (DBS) to treat motor disorders in Parkinson's disease (PD) (see Benabid [1] for a review) and neuropsychiatric diseases, such as Tourette's syndrome [2], is now widely accepted. PD is a neurodegenerative disease that gradually

---

J. Modolo (✉) · A. Beuter  
Laboratoire Intégration du Matériau au Système, CNRS UMR 5218,  
Université Bordeaux 1, Talence, France  
e-mail: modolo@idc.u-bordeaux2.fr

J. Henry  
INRIA Bordeaux Sud-Ouest, Institut de Mathématiques de Bordeaux,  
Université Bordeaux 1, Talence, France

destroys the dopaminergic neurons in the Substantia Nigra pars compacta (SNc). This dopaminergic deficiency leads to abnormally synchronised, low-frequency activity in several brain areas. Consequently, motor function is impaired and symptoms such as tremor, rigidity, bradykinesia, and postural instability are observed [3]. Nowadays, the only treatments for PD are symptomatic, including L-Dopa uptake or DBS (National Institute for Neurological Disorders and Stroke, <http://www.ninds.nih.gov>). In PD, this non-destructive, reversible, but invasive neurosurgical procedure, during which the patient is awake, consists of placing a macroelectrode in the subthalamic nucleus (STN), a small, almond-shaped nucleus belonging to the basal ganglia. The stimulator itself, implanted in the chest wall of the patient, delivers high-frequency electrical stimulation (typically above 100 Hz). The battery has a lifetime of about 45 months [4]. The stimulation parameters (amplitude, pulse width and frequency) are adjusted by telemetry and modified regularly to maintain clinical improvement despite the evolution of the disease. DBS significantly reduces the amount of medication (L-Dopa) needed to alleviate the symptoms [3]. Interestingly, although about 40,000 people worldwide benefit from DBS [5]; the origin of its clinical benefits is still largely unexplained. However, several hypotheses have been proposed, including (1) depolarisation block, in which the strong DBS current disrupts ionic currents, preventing the triggering of action potentials [6]; (2) neuronal jamming, suggesting that the information carried by the stimulated network is so strongly perturbed that this information becomes meaningless [1]; (3) functional inhibition of the stimulated structure [7]; and (4) disruption of pathological network activity [7, 8]. The picture that emerges is that DBS replaces a pathological brain activity (abnormal synchronisation) in several brain substructures by a new activity, more compatible with the satisfactory processing of sensorimotor signals [9]. Recent, innovative DBS stimulation protocols, such as coordinated delayed feedback of neuronal populations [10, 11], have suggested that DBS desynchronises neuronal activity in the STN. The explanation is not so clear for standard DBS stimulation protocols, which involve chronic, high-frequency electrical stimulation.

The reversibility of PD symptoms [12] led Beuter and Vasilakos [13] to qualify PD as a dynamical disease. Mackey and Glass [14] defined a dynamical disease as abnormal dynamics appearing when a control parameter, e.g., the concentration of a hormone or neurotransmitter, is out of range. In PD, the main control parameter is apparently dopamine concentration, which decreases as the disease progresses. When the first clinical symptoms of the disease appear, 60% to 80% of the dopaminergic neurons in the SNc have already degenerated [15].

There are several functionally segregated, parallel loops, linking the cortex to the basal ganglia, then the thalamus, and back to the cortex [16]. One of the loops affected in PD is the motor loop. The complex formed by the STN and the external segment of the Globus Pallidus (GPe) is thought to induce a “pacemaker-like” activity in this motor loop [17]. An illustration of this pacemaker-like effect is the switching of activity in this network between the healthy and diseased states, from a weak, uncorrelated activity to a strong, oscillatory activity [17–19]. The strong oscillations in the subthalamo-pallidal complex are assumed to “drive” the motor loop at a low-frequency (3–8 Hz), oscillatory regime, not compatible with satisfactory processing of motor information relayed by the thalamus [20]. Computational models developed by Gillies and Willshaw [19], as well as Terman et al. [18], showed that the STN–GPe complex exhibited different dynamics depending on the connectivity pattern and striato-pallidal inhibition.

Approaching this problem from a dynamical perspective, Titcombe et al. [21] analysed tremor dynamics in patients with PD receiving DBS in the STN, the internal segment of

the Globus Pallidus (GPi), or the ventral intermediate thalamus (Vim) [22], and found that a supercritical Hopf bifurcation occurred in tremor dynamics when DBS was switched “on”. The bifurcation parameter was assumed to be related to a time-dependent amount of neurotransmitter released during stimulation pulses. STN activity has been shown to be tightly correlated with tremor dynamics [20, 23], which may suggest the presence of a bifurcation in STN dynamics similar to the one in tremor dynamics. Thus, DBS may switch the dynamical regime from a pathological to a more favourable one (in terms of thalamic relay performance) via a second bifurcation. In that case, DBS would be, in some sense, a bifurcation control-based treatment.

One difficulty in understanding the effects of DBS on the stimulated structure is due to the analysis of multiple recordings of spike trains. Indeed, DBS current causes important artefacts in neuronal activity recordings. However, refinements in experimental techniques have resulted in “artefact-free” neuronal recordings in rat brain slices [9], and even local field potential in patients with PD receiving DBS [24]. The problem is that, in brain slices, the connectivity between subcortical structures is incomplete, as many axons are cut during slice preparation. Thus, it is safe to say that in vivo neuronal activity in patients receiving DBS is likely to differ from multi-site recordings in rat brain slices to which a DBS current is applied. Consequently, until new experimental protocols become available, the modelling approach represents a useful alternative for investigating neuronal activity in the stimulated structure during DBS in PD patients. Therefore, the goal of this paper is to compare two different modelling approaches for exploring the dynamics of the subthalamo-pallidal complex subjected to various DBS currents. The first was a simple firing-rate model, which revealed several limitations in understanding the effects of DBS in PD. The second, population-based, model reproduced neuronal dynamics more faithfully.

## 2 Mathematical Models

### 2.1 Firing-rate Model

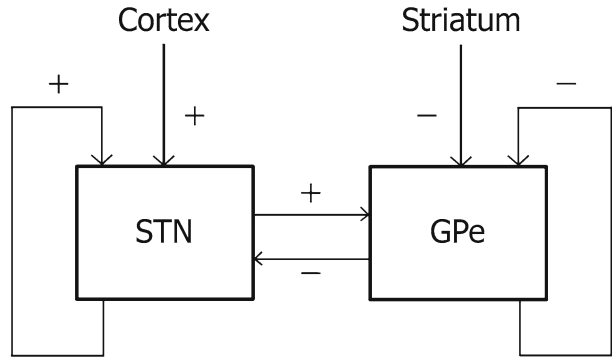
We extended the simple firing-rate model proposed by Gillies and Willshaw [19] by applying a high-frequency stimulation current to the STN. Indeed, in its original form, this model did not address the DBS issue. The subthalamo-pallidal dynamical model proposed by Gillies and Willshaw [19] consisted of a set of two coupled differential equations describing variations in mean STN and GPe potentials [25]

$$\tau^{\text{STN}} \frac{d}{dt} x = -x + \bar{a}\sigma(x) - \bar{c}\zeta(y) + I^{\text{Cx}} \quad (1)$$

$$\tau^{\text{GPe}} \frac{d}{dt} y = -y - \bar{b}\zeta(y) + \bar{d}\sigma(x) + I^{\text{Str}} \quad (2)$$

where  $x$ ,  $y$  expressed in millivolts are the mean membrane potentials in STN and GPe cells, respectively,  $\bar{a}$ ,  $\bar{b}$ ,  $\bar{c}$ ,  $\bar{d}$ , expressed in microvolts per Hertz, are the connectivity parameters between and within the STN and GPe ( $a$ ,  $b$ ,  $c$ ,  $d$  in Gillies and Willshaw [19], modified to avoid confusion with the parameters of the Izhikevich model, see below), and  $I^{\text{Cx}}$ , and  $I^{\text{Str}}$  (in millivolts) represent inputs from the cortex and striatum, respectively. Excitatory and inhibitory relationships are illustrated in Fig. 1.

**Fig. 1** Schematic view of the network formed by the STN and GPe. *Plus* and *minus* signs denote excitatory and inhibitory relationships, respectively



Finally,  $\sigma(x)$  and  $\zeta(y)$ , expressed in Hertz, are the STN and GPe firing rates, respectively (number of action potentials per cell per unit of time, related to the mean membrane potential via a sigmoid function), and are expressed as [19]

$$\sigma(x) = \frac{\sigma_{\max}}{1 + \exp(-\kappa(x - x_{\text{th}}))} \tag{3}$$

$$\zeta(y) = \frac{\zeta_{\max}}{1 + \exp(-\eta(y - y_{\text{th}}))} \tag{4}$$

with  $\sigma_{\max} = 500$  Hz,  $\zeta_{\max} = 100$  Hz,  $\kappa = 0.3 \text{ mV}^{-1}$ ,  $\eta = 0.2 \text{ mV}^{-1}$ ,  $x_{\text{th}} = 15$  mV, and  $y_{\text{th}} = 10$  mV [19]. Thus, mean membrane potentials are computed first, followed by the firing rate for each population, using the two sigmoid functions in (3) and (4). As in the general case of an excitatory–inhibitory neuronal network, the subthalamo-pallidal complex exhibits two different types of dynamical regime in this computational model: stable and limit cycle behaviours [26]. In the stable regime, the system goes back to the rest equilibrium after a stimulus [27], whereas, in the limit cycle regime, the trajectory converges to a closed orbit in the phase space. The main parameter controlling the transition from healthy to pathological activity is the level of striato-pallidal inhibition,  $I^{\text{str}}$ . Indeed, the level of striato-pallidal inhibition increases following dopaminergic depletion and is associated with the release of enkephalin and dynorphin, which weaken intra-GPe synapses [18].

A typical DBS current depends on pulse amplitude, frequency, and width. It is modelled by a train of square impulses. The parameter values proposed in Gillies and Willshaw [19] are used to simulate a pathological (low-frequency, oscillatory) behaviour of the subthalamo-pallidal complex, i.e.,  $\bar{a} = 54 \text{ } \mu\text{V Hz}^{-1}$ ,  $\bar{b} = 100 \text{ } \mu\text{V Hz}^{-1}$ ,  $\bar{c} = 120 \text{ } \mu\text{V Hz}^{-1}$ ,  $\bar{d} = 80 \text{ } \mu\text{V Hz}^{-1}$ ,  $I^{\text{cx}} = 9$  mV and  $I^{\text{str}} = 13$  mV. The time constants of STN and GPe neurons are  $\tau_{\text{STN}} = 6$  ms and  $\tau_{\text{GPe}} = 14$  ms, respectively [19]. The DBS current is included in the evolution equation for the STN by adding the term  $I^{\text{DBS}}(t)$  in (1). We numerically integrated this system of differential equations using a first-order Euler method.

## 2.2 Population-based Model of the Subthalamo-pallidal Complex

We considered the complex formed by the STN and GPe, with recurrent and feedforward connectivity. The addition of recurrent connectivity within the STN differs from the Terman et al. model [18], while Gillies and Willshaw [19] found it highly relevant for understanding basal ganglia dynamics. In our model, both nuclei are described by a population-density

function  $p(\vec{w}, t)$  where  $\vec{w} = (v, u)$  is the state of the neuron,  $v$  and  $u$  are the state variables from the Izhikevich model [28], and  $t$  is the time [29, 30]. This function is such that  $\int \int p(\vec{w}, t) d\vec{w} = N$ , where  $N$  is the number of neurons in the population ( $\approx 2 \times 10^5$  for the STN [31] and for the GPe) and  $p(\vec{w}, t) d\vec{w}$  is the number of neurons in  $[w, w + dw]$ . The initial condition for the population-density function is in the form of a Gaussian function [30]. The evolution of this function for one neural population is given by the following conservation law [32]:

$$\frac{\partial}{\partial t} p(\vec{w}, t) = -\vec{\nabla} \cdot \vec{J}(\vec{w}, t) \tag{5}$$

where the *neuronal flux* term  $\vec{J}(\vec{w}, t)$  can be expressed as the sum of two terms: one for internal dynamics (streaming term) and one for imposed dynamics, such as synaptic events (interaction term). These terms may be written as

$$\vec{J}_s(\vec{w}, t) = p(\vec{w}, t) \vec{F}(\vec{w}) \tag{6}$$

$$\vec{J}_{int}(\vec{w}, t) = \hat{e}_v \sigma(t) \int_{v-\epsilon}^v p(\vec{v}, u, t) d\vec{v} \tag{7}$$

where  $\vec{F}(\vec{w}) = (F_v, F_u)$  is the Izhikevich model [28] that includes four parameters  $a, b, c, d$ , where

$$F_v = \frac{dv}{dt} = 0.04v^2 + 5v + 140 - u + I(t) + I^{str}(t) \tag{8}$$

$$F_u = \frac{du}{dt} = a(bv - u) \tag{9}$$

$$v > 30 \text{ mV} \rightarrow v = c, u = u + d \tag{10}$$

and  $\epsilon$ , expressed in millivolts, is the amplitude of the EPSP/IPSP (excitatory/inhibitory post-synaptic potential), assumed to be instantaneous;  $\sigma(t)$ , expressed in Hertz, is the average spike reception rate per neuron;  $\hat{e}_v$  is a unitary vector in the  $v$  direction; and  $I^{str}(t)$  (in picoamperes) is the striatal inhibitory input applied to GPe cells. Let us note that the parameters  $a, b, c, d$  completely define the Izhikevich model. The dynamics of STN and GPe neurons are described by the following system of partial differential equations for an excitatory–inhibitory network [29], where the population-density function for each structure follows (5) above:

$$\begin{aligned} \frac{\partial}{\partial t} p_{STN}(\vec{w}, t) = & -\vec{\nabla} \cdot \left\{ \vec{F}_{STN}(\vec{w}) p_{STN}(\vec{w}, t) \right. \\ & + \vec{e}_v \left[ \sigma_{exc}^{STN}(t) \int_{v-\epsilon}^v p_{STN}(\vec{w}, t) d\vec{v} - \sigma_{inhib}^{GPe}(t) \right. \\ & \left. \left. \times \int_v^{v+\epsilon} p_{STN}(\vec{w}, t) d\vec{v} \right] \right\} \end{aligned} \tag{11}$$

$$\begin{aligned} \frac{\partial}{\partial t} p_{\text{GPe}}(\vec{w}, t) = & -\vec{\nabla} \cdot \left\{ \vec{F}_{\text{GPe}}(\vec{w}) p_{\text{GPe}}(\vec{w}, t) \right. \\ & + \vec{e}_v \left[ \sigma_{\text{exc}}^{\text{STN}}(t) \int_{v-\epsilon}^v p_{\text{GPe}}(\vec{w}, t) d\vec{v} - \sigma_{\text{inhib}}^{\text{GPe}}(t) \right. \\ & \left. \left. \times \int_v^{v+\epsilon} p_{\text{GPe}}(\vec{w}, t) d\vec{v} \right] \right\} \end{aligned} \tag{12}$$

where  $\sigma_{\text{exc}}(t)$  and  $\sigma_{\text{inhib}}(t)$  are the mean individual reception rates of excitatory/inhibitory inputs, respectively, expressed as a function of STN and GPe firing rates. For a single population with a constant axonal delay  $\tau$ ,  $\sigma(t)$  is expressed as

$$\sigma(t) = \frac{W}{N} r(t - \tau) \tag{13}$$

where  $W$  is the mean number of afferent connections per neuron,  $N$  is the total number of neurons in the population, and  $r(t)$  is the total firing rate of the population at time  $t$ , computed as the flux in the  $v$  direction through the  $v = 30$  mV boundary, so that

$$r(t) = \int \frac{dv}{dt} \Big|_{v=30} p(s, u, t) du. \tag{14}$$

The system of conservation equations is solved using the finite-volumes-based numerical scheme described in Modolo et al. [30].

For the sake of neurophysiological plausibility, we adjusted the Izhikevich model to exhibit similar responses to those recorded experimentally in STN projection neurons. Then, the corresponding term  $\vec{F}(\vec{w})$  was included in the population-based model. The main neurophysiological features of STN neurons, according to Bevan and Wilson [33], are (1) a spontaneous spiking activity between 3 and 20 Hz; (2) increased spiking activity in response to an excitatory input current; and (3) a post-inhibitory rebound burst followed by a quiescence period, caused by the inactivation of the low-threshold  $\text{Ca}^{2+}$  current. The membrane potential variation in response to excitatory and inhibitory inputs, respectively, in our modified Izhikevich model, is presented in Fig. 2.

**Fig. 2** Variation in membrane potential for an STN projection neuron, based on the Izhikevich model, defined by  $(F_v, F_u)$ , with a new set of parameters:  $a = 0.005, b = 0.265, c = -65, d = 1.5$  [used in (9) and (10)]

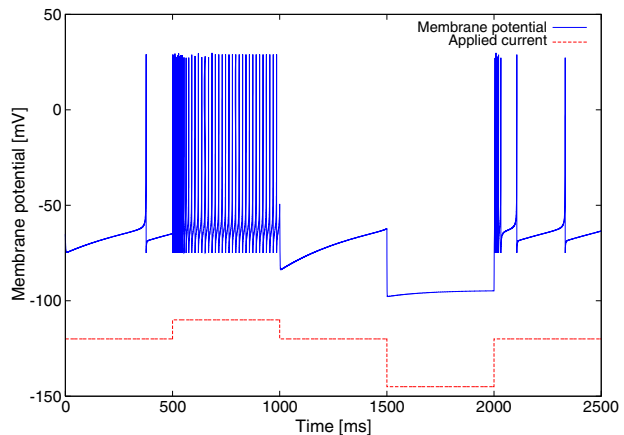


Figure 2 shows that this new discharge mode of the Izhikevich model matches the main STN neurophysiological features listed above. Consequently, we used these parameter values in our main population equation (conservation law) to simulate a population of STN glutamatergic projection neurons. GABAergic GPe neurons were modelled using the set of parameters defined as *fast spiking* by Izhikevich [28] ( $a = 0.1$ ,  $b = 0.2$ ,  $c = -65$ ,  $d = 2$ ). The fast-spiking regime has similar parameters to the *low-threshold spiking* regime, both exhibited by inhibitory neurons [28]. This simple model for GPe neurons did not include a post-inhibitory rebound, as it was not necessary to generate STN–GPe oscillations [20]. The amplitudes of instantaneous EPSPs and IPSPs were equal in absolute value, namely  $\epsilon = 1$  mV. The DBS current  $I^{\text{DBS}}(t)$  was applied directly to the neuronal membrane in the STN neuron model.

$$\frac{dv}{dt} = 0.04v^2 + 5v + 140 - u + I^{\text{str}}(t) + I^{\text{DBS}}(t) \quad (15)$$

$$\frac{du}{dt} = a(bv - u) \quad (16)$$

This is justified by experimental evidence that DBS excites STN neuron membranes [34].

### 3 Results

#### 3.1 Simulations with a Firing-rate Model

The objective was to investigate the effect of stimulation frequency on the dynamical behaviour of the STN–GPe complex. Initially, we did not include the DBS current and used the set of parameters presented by Gillies and Willshaw [19] to simulate pathological behaviour of the subthalamo-pallidal complex. Throughout the paper, the term “phase diagram” describes a graph plotting “STN activity” vs “GPe activity”. The activity and phase diagram of the STN–GPe complex with this set of parameters are shown in Fig. 3.

Figure 3 (right) shows that, in PD, the subthalamo-pallidal complex exhibits a limit cycle, with a 5-Hz oscillation frequency similar to the tremor frequency, as shown in Fig. 3 (left). Furthermore, experimental evidence indicates a correlation between tremor bursts and the abnormal oscillations in the STN [23]. This empirical relationship between bursting activity

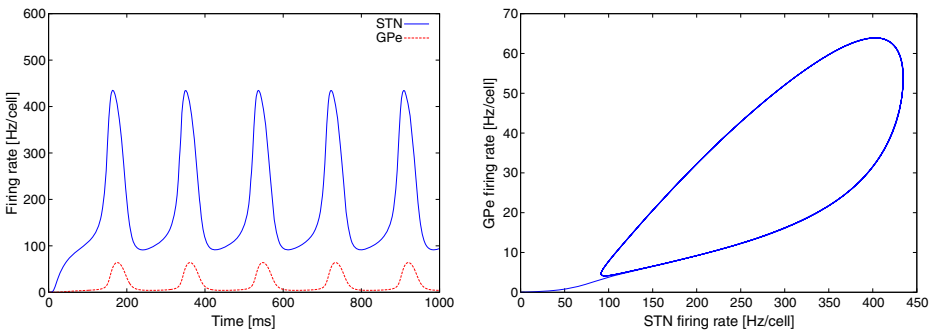


**Fig. 3** STN and GPe activity firing rates in the pathological case (*left*) in the firing-rate model proposed by Gillies and Willshaw [19]. The system no longer displays a stable stationary state but instead exhibits a limit cycle (*right*)

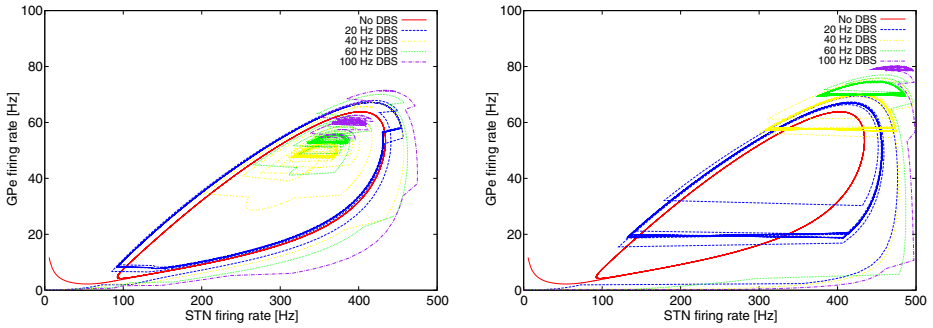


**Fig. 4** Effect of DBS current frequency on the phase plane of the STN–GPe complex for  $I_0 = 100$  mV (*left*) and  $I_0 = 500$  mV (*right*)

in STN cells and tremor is used below in Section 3 to provide a rough qualitative estimate of tremor modulation during DBS.

In the following simulations, we applied a DBS current in the form of a monophasic square-pulse train to the STN, using a pulse width of  $150 \mu\text{s}$  (therapeutic value) and an amplitude from  $I_0 = 100$  to  $2,000$  mV. The pulse frequency was increased gradually from 20 to 200 Hz. In clinical practice, only stimulation frequencies higher than, or equal to, 100 Hz are used.

Interestingly, these simulations showed that a low-frequency DBS current still produced limit cycle behaviour (with large amplitude) in the subthalamo-pallidal complex. This is consistent with experimental observations, reporting that low-frequency DBS does not improve, but can actually worsen, motor symptoms [35, 36]. A new dynamical behaviour emerges in subthalamo-pallidal complex activity at therapeutic stimulation pulse amplitudes (between 1 and 2 V) and high frequencies, as shown on the phase plane plots (Figs. 4 and 5). In fact, this is still a limit cycle, but the amplitude tends towards 0. Thus, this high-activity state is described as a “quasi-stationary” state. These findings suggest that DBS switches the dynamical regime to a quasi-stationary, high-activity state (different from the healthy state that is stationary with low activity), thus breaking the limit cycle regime imposed by the evolution of the disease, i.e., the increase in striato-pallidal inhibition, among other factors.

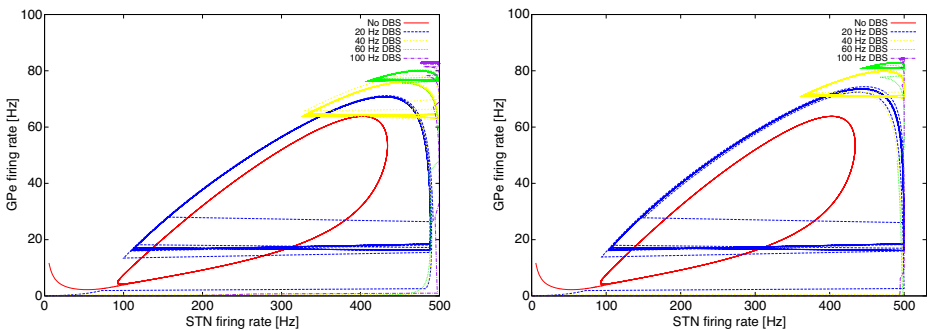


**Fig. 5** Effect of DBS current frequency for  $I_0 = 1,000$  mV (*left*) and  $I_0 = 2,000$  mV (*right*) on the phase plane of the STN–GPe complex

### 3.2 Simulations using a Population-based Model

The population-based model presented in Section 2 was used to simulate the STN–GPe complex, by means of a system of partial differential equations [29]. In the remaining section of the paper, “healthy state” refers to a weak, almost constant activity in the subthalamo-pallidal complex and “pathological state” refers to low-frequency, high-amplitude, oscillatory activity. It is possible to switch from a healthy to a pathological state by increasing the constant striato-pallidal inhibition level. We illustrate this in our population-based model with two different levels of striato-pallidal inhibition, which impact the activity pattern of the STN–GPe complex. The recurrent connectivity pattern is  $W_{\text{STN} \rightarrow \text{STN}} = 50$ ,  $W_{\text{GPe} \rightarrow \text{GPe}} = 25$  synaptic afferent connections per neuron, feedforward connectivity  $W_{\text{STN} \rightarrow \text{GPe}} = 15$ ,  $W_{\text{GPe} \rightarrow \text{STN}} = 15$ , with an EPSP/IPSP amplitude of 1 mV in absolute value. Time delays caused by axonal conduction were 1 ms for all connections. The results of these simulations are presented in Fig. 6, where the firing rate is defined as the number of spikes per time unit per cell.

Consistent with experimental data [37], increasing striato-pallidal inhibition gradually caused synchronous activity between the STN and GPe, with a tendency towards bursting. DBS current was then applied to the STN with the subthalamo-pallidal complex in a pathological state, by adding a term consisting of DBS pulses, width  $\Delta = 150 \mu\text{s}$ , in a frequency range from 20 to 100 Hz, with a pulse amplitude of 250 pA. The activity of the subthalamo-pallidal complex at different stimulation frequencies is presented in Fig. 7.

These simulations showed that low-frequency DBS (e.g., 20 Hz DBS, Fig. 7, top left) had no major effect on the subthalamo-pallidal pattern, which remained in a low-frequency, bursting mode. However, it did affect the frequency, as activity bursts became phase-locked with DBS pulses. As mentioned above, the bursting activity of STN neurons is associated with the presence of symptoms. Thus, our results are qualitatively consistent with the observations that patients with PD who received low-frequency DBS did not experience any improvement in motor symptoms, which even worsened in some cases [35, 36].

In contrast, the bursting activity of the STN disappeared under high-frequency DBS current (100 Hz and above). Thus, the effect of gradually increasing the stimulation frequency was to reduce pathological bursting activity in the STN and promote tonic activity. Interestingly, in our population-based model, the DBS frequency that evoked tonic

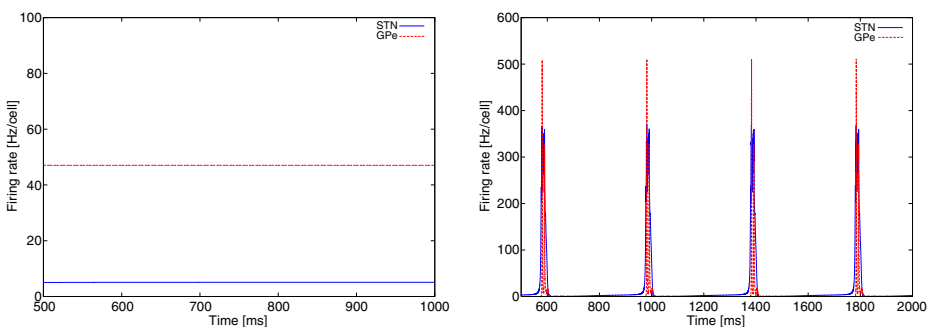


**Fig. 6** Impact of striato-pallidal inhibition levels ( $I^{\text{Str}} = 0$ —left, physiological state— and  $I^{\text{Str}} = -5 \text{ pA}$ —right, pathological state) on the activity pattern of the STN–GPe complex in the population-based model

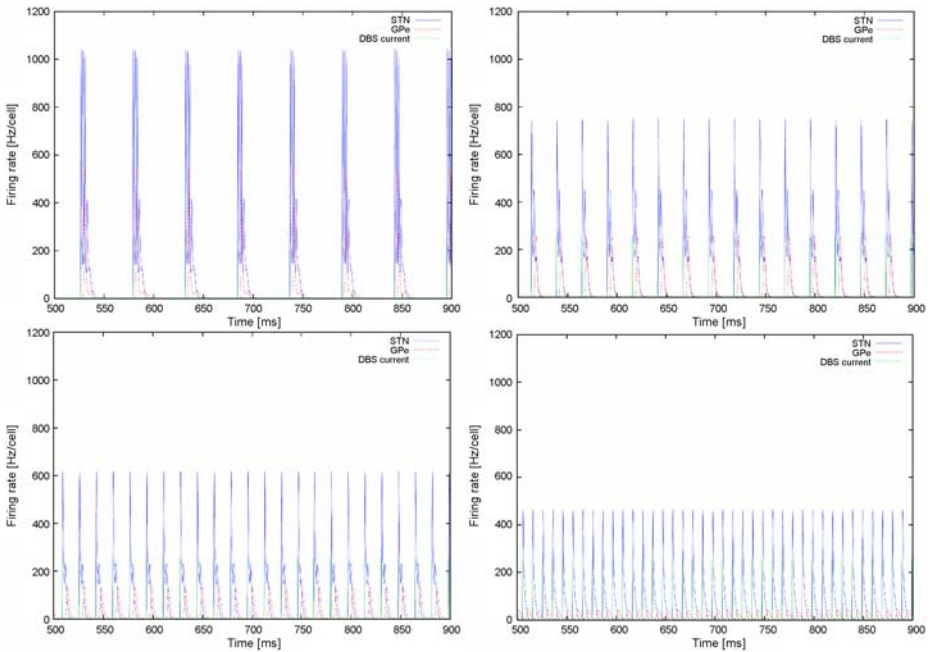


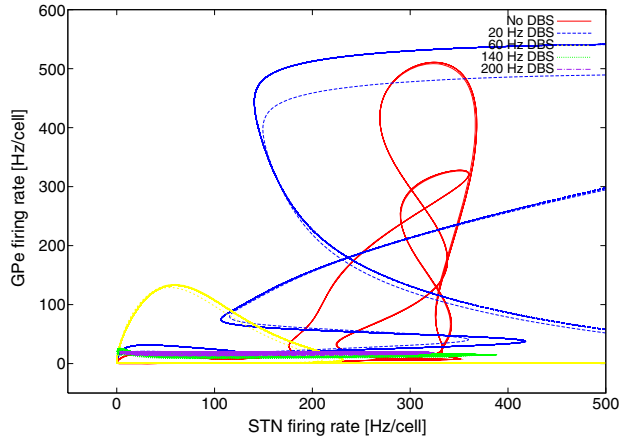
**Fig. 7** Effect of DBS current frequency on the mean firing rate per cell in the STN–GPe complex: 20 Hz (top, left), 40 Hz (top, right), 60 Hz (bottom, left) and 100 Hz (bottom, right)

STN activity (100 Hz) was on the order of magnitude of stimulation frequencies used in DBS in patients with PD (120–180 Hz, Benabid [1]).

A phase plane plot for the mean firing rate per STN/GPe cell at different stimulation frequencies (20 to 100 Hz) is presented in Fig. 8 (for the sake of clarity, only results obtained at  $I = 250$  pA are presented). As seen in Fig. 8, the limit cycle was more complex than that obtained with the firing-rate model. This was due to the greater accuracy in describing individual unit dynamics in the population-based model. However, this phase plot for STN–GPe activity shares a common feature with the results obtained using the firing-rate model, i.e., the amplitude of the STN–GPe complex limit cycle decreased significantly as stimulation frequency increased. The limit attractor for higher frequencies was apparently a limit cycle with a much smaller amplitude than in the pathological case (i.e., without DBS).

The phase plane representation of STN–GPe activity was similar to the phase plane generated with the firing-rate model. The amplitude variations in GPe activity were smaller than in STN activity and the amplitude of the limit cycle was smaller at high stimulation frequencies (Figs. 5 and 7). Furthermore, low stimulation frequencies (e.g., 20 Hz) increased the limit cycle amplitude in both models. This result was similar to driven oscillations: when a system is forced at stimulation frequencies close to its intrinsic (near resonance), the system response amplitude increases, whereas, at higher frequencies, the system is driven with a smaller response amplitude. However, we observed considerable differences between the two models, commented on in Section 4. Interestingly, at high stimulation frequencies, GPe activity decreased markedly in the population-based model, and the STN had a high-frequency, tonic activity.

**Fig. 8** Effect of DBS current frequency on the phase plane of the STN–GPe complex in the population-based model



Variations in STN response to DBS at frequencies between 5 and 180 Hz were systematically investigated, as shown in Fig. 9. The differential response is defined as the ratio of the maximum firing rate during one activity burst of the STN, in response to one DBS pulse, to the maximum firing rate during one activity burst without DBS.

As seen in Fig. 9, the 10-Hz DBS current resonates with the intrinsic frequency of STN neurons. Thus, it tends to exacerbate pathological activity in the same frequency range, possibly explaining why low-frequency DBS is ineffective. We suggest that the differential effects of DBS at different stimulation frequencies are due to a possible resonance between the stimulating frequency and the eigen frequency of STN neurons. This observation suggests that, for future applications of DBS targeting other structures, resonant stimulation frequencies should be avoided to prevent possible exacerbation of pathological activity. This can be achieved by measuring the eigen frequencies of target structures.

**Fig. 9** Differential response of modelled STN neurons to DBS currents at varying frequencies

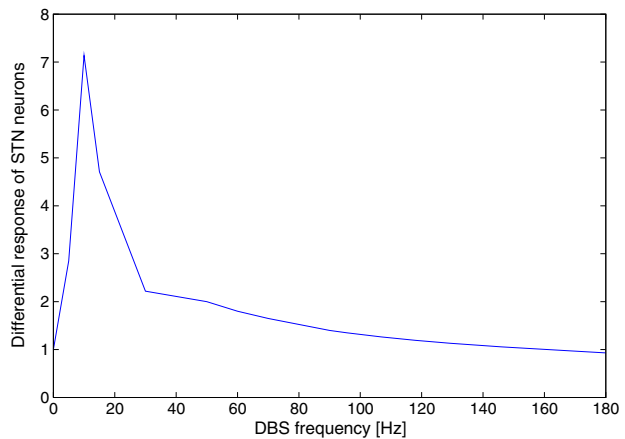
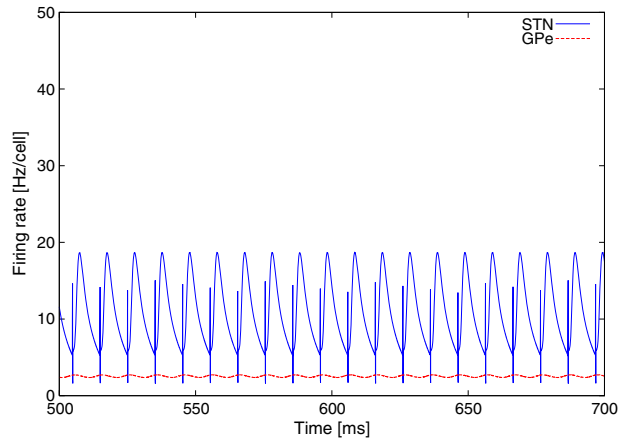


**Fig. 10** Activity of the subthalamo-pallidal complex under biphasic, charge-balanced stimulation current at 100 Hz



### 3.3 Case of Biphasic Stimulation Current

Previous simulations investigated the dynamics of the subthalamo-pallidal complex under external stimulation by DBS current, modelled as a train of simple square pulses (e.g., Rubin and Terman, [20]). However, in practice, DBS stimulators use either monopolar or bipolar stimulation mode. In monopolar mode, the stimulator device plays the role of the anode and one of the four active contacts of the DBS electrode acts as the cathode. In bipolar mode, one of the active contacts is the anode and another plays the role of cathode. Furthermore, stimulation pulses can be monophasic (only a positive or negative pulse) or biphasic (a positive or negative pulse, followed by a negative or positive pulse, respectively). Monophasic stimulation may cause an accumulation of charges in neural tissue, potentially leading to tissue damage [38]. During charge-balanced, biphasic stimulation (such as those used currently in DBS), pulses with negative and positive components of equal amplitude are applied in turn. Consequently, we tested a biphasic, charge-balanced DBS current with a pulse width of 150  $\mu$ s (the first half of the pulse was positive and the second negative) and a pulse amplitude of absolute value 250 pA, at a frequency of 100 Hz. The activity pattern was qualitatively similar to that obtained using monophasic current, with a considerable reduction in the amplitude of neuronal activity in both the STN and GPe, as shown in Fig. 10. Thus, future models should be tested using more realistic biphasic, charge-balanced stimulation currents, as the results differ markedly depending on the pulse form.

## 4 Discussion

This section discusses the similarities and differences observed between two mathematical models used to investigate the dynamics of the subthalamo-pallidal complex under low- and high-frequency DBS. It then examines the effect of two different current types and, finally, offers a possible interpretation of the effect of DBS on the subthalamo-pallidal complex.

The results of the firing-rate and population-based models show some similarities, but also several important differences. First, the GPe appeared more active in the firing-rate than the population-based model. This issue does not seem relevant, however, as these

approaches use very different ways of implementing neuronal coupling. Second, the limit cycle of activity for the subthalamo-pallidal complex during high-frequency electrical stimulation is much smaller in the firing-rate model. This is due to an intrinsic limitation of firing-rate models, which are unable to capture fast transients [32], and DBS pulses are certainly very short (time scale, 100  $\mu$ s). The network input is assumed to vary slowly in firing-rate models, which is obviously not the case for DBS pulses, where DBS current switches instantaneously from zero to a high value. Thus, the firing-rate model may miss the fast response of STN neurons to stimulation, which are, however, captured by the population-based model. This results in a larger limit cycle in the population-based model. Indeed, the firing-rate model indicated a roughly constant firing rate at  $\approx 500$  Hz, whereas the population model revealed a more complex picture of short, high-frequency responses to DBS. Population models, unlike firing-rate models, are independent of network input (DBS pulses) variation rates. Third, individual neuron dynamics are taken into account in a radically different manner. In firing-rate models, a sigmoid function provides the relationship between the mean neuron membrane potential and the firing rate. However, in the population-based model, neuron dynamics are given by the Izhikevich model, more accurately reflecting the dynamical response of neurons to stimulation. In contrast, the simple membrane potential-firing rate sigmoid function of firing-rate models cannot describe a post-inhibitory response, a major characteristic of STN cells. Finally, firing-rate models are limited in their description of synchronised population dynamics [26].

In summary, although firing-rate models provide some useful information, they are inappropriate for understanding dynamical phenomena on such small-time scales. In line with experimental observations [9], the results of our population-based model show that the STN switches from pathological, bursting activity to regular, tonic activity in response to high-frequency DBS. On the contrary, both models found that low-frequency DBS exacerbated low-frequency oscillatory activity in the STN, which is consistent with previous experiments [35] and modelling [20]. Thus, when the stimulation frequency is increased, the bursting behaviour gradually disappears and is replaced by tonic activity at high frequencies. This suggests that a bifurcation in STN activity occurs when high-frequency DBS is switched on. Experimental findings [17] and modelling studies [18] revealed that oscillatory activity in the subthalamo-pallidal complex was subject to two conditions: (1) an increase in striato-pallidal inhibition and (2) a weakening of intrapallidal connections. The population model results are consistent with these findings, even if the weakening of intra-GPe connections was not investigated.

The results obtained in the population-based model with monophasic stimulation current suggest a possible explanation for the paradox that similar improvements in motor symptoms are observed with both subthalamotomy (STN lesion) and STN high-frequency stimulation. Functional models are unable to resolve this paradox as they cannot explain how a lesion (irreversible destruction) has similar effects to high-frequency stimulation, assumed to excite STN neurons and increase their activity. In our dynamical system approach, we assume that the STN can hardly respond to external inputs (e.g., cortical afferences), as our results indicate that DBS causes a sort of saturation in neuronal activity. If the STN is incapable of responding to external inputs during DBS, then is it really different from a lesion, which also prevents the STN from responding to external inputs? One obvious difference is that the STN output has a high frequency and is tonic during DBS, but nonexistent after a lesion. In fact, tonic activity of the STN–GPe complex is associated with a tonic inhibition of the thalamus by the GPi [20]. Furthermore, this tonic activity takes place in the  $\gamma$  band (30 to 80 Hz), associated with voluntary movements [39].

Thus, the high-frequency, tonic STN activity in the  $\gamma$  band is compatible with appropriate sensorimotor signal processing by the thalamus. However, this conclusion was disproved by the effects of biphasic, charge-balanced stimulation current, highlighting the importance of using an appropriate stimulation current type in simulation studies.

Our results suggest the following scenario: when the STN is stimulated at high frequencies, its tonic output strongly activates GPe cells that inhibit each other via their collaterals. This explains why, in our simulations, GPe cell activity was weak during DBS. This is qualitatively consistent with experimental findings revealing a slight decrease in GPe cell activity during DBS [40]. The STN and GPe are the two main afferent inputs to the GPi, a structure that sends inhibitory projections to the thalamus. In PD, GPi cells exhibit an abnormal, low-frequency bursting activity, similar to that found in the STN or GPe. GPi cells have the same post-inhibitory rebound feature as STN and GPe neurons. Therefore, we hypothesise that, during DBS, the decrease in GPe activity weakens GPi inhibition, as well as post-inhibitory rebounds in GPi cells. Combined with a tonic, high-frequency input from the STN, this decrease reduces or suppresses bursting activity in GPi cells and causes a high-frequency, tonic driving in GPi cells. Interestingly, GPi and STN DBS produce slightly different motor improvements in PD patients (for an example concerning tremor, see Beuter et al. [41]).

## 5 Concluding Remarks

This study focuses on STN and GPe dynamics during DBS. Of course, the interactions of these structures with other nuclei in the motor loop, such as the GPi, thalamus or motor cortex, may also impact the behaviour of the subthalamo-pallidal complex. However, the role of this complex appears highly relevant to understanding rhythm generation in the motor loop. One interesting prospect is to extend this subthalamo-pallidal complex model by “closing the loop” with a population of cortical cells and exploring the interactions between these two populations. Cortical stimulation to control basal ganglia dynamics may offer an alternative, less invasive treatment for motor symptoms in PD, despite the fact that experimental results have not yet been convincing [42].

**Acknowledgements** This work was supported by the European Network of Excellence BioSim (contract No. LSHB-CT-2004-005137) and the Aquitaine Region (convention No 20051399003). We thank André Garenne, Christian Hauptmann and Axel Hutt for useful comments in the preparation of the manuscript.

## References

1. Benabid, A.L.: Deep brain stimulation for Parkinson's disease. *Curr. Opin. Neurobiol.* **13**, 696–706 (2003)
2. Visser-Vanderwalde, V.: DBS in Tourette syndrome: rationale, current status and future prospects. *Acta Neurochir.* **97**, 215–222 (2007)
3. Hamani, C., Richter, E., Schwab, J.M., Lozano, A.M.: Bilateral subthalamic nucleus stimulation for Parkinson's disease: a systematic review of the clinical literature. *Neurosurgery* **56**(6), 1313–1324 (2005)
4. Bin-Mahfooth, M., Hamani, C., Sime, E., Lozano, A.M.: Longevity of batteries in internal pulse generators used for deep brain stimulation. *Stereotact. Funct. Neurosurg.* **80**(1–4), 56–60 (2003)
5. Pereira, E.A.C., Green, A.L., Nandi, D., Aziz, T.Z.: Deep brain stimulation: indications and evidence. *Expert Rev. Med. Devices* **4**, 591–603 (2007)

6. Beurrier, C., Bioulac, B., Audin, J., Hammond, C.: High-frequency stimulation produces a transient blockade of voltage-gated currents in subthalamic neurons. *J. Neurophysiol.* **85**, 1351–1356 (2001)
7. McIntyre, C.C., Savasta, M., Kerkerian-Le Goff, L., Vitek, J.L.: Uncovering the mechanism(s) of action of deep brain stimulation: activation, inhibition, or both. *Clin. Neurophysiol.* **115**, 1239–1248 (2004)
8. Montgomery, E.B., Gale, J.T.: Mechanisms of deep brain stimulation: implications for physiology, pathophysiology and future therapies. In: 10th Annual Conference of the International FES Society, Montreal, 5–8 July 2005
9. Garcia, L., D'Alessandro, G., Bioulac, B., Hammond, C.: High-frequency stimulation in Parkinson's disease: more or less? *Trends Neurosci.* **28**, 209–216 (2005)
10. Tass, P.A.: A model of desynchronizing deep brain stimulation with a demand-controlled coordinated reset of neural subpopulations. *Biol. Cybern.* **89**, 81–88 (2003)
11. Hauptmann, C., Popovych, O., Tass, P.A.: Effectively desynchronizing deep brain stimulation based on a coordinated delayed feedback stimulation via several sites: a computational study. *Biol. Cybern.* **93**, 463–470 (2005)
12. Levy, R., Lang, A.E., Dostrovsky, J.O., Pahapill, P., Romas, J., Saint-Cyr, J., Hutchison, W.D., Lozano, A.M.: Lidocaine and muscimol microinjections in subthalamic nucleus reverse Parkinsonian symptoms. *Brain* **124**, 2105–2118 (2001)
13. Beuter, A., Vasilakos, K.: Tremor: is Parkinson's disease a dynamical disease? *Chaos* **5**, 35–42 (1995)
14. Mackey, M.C., Glass, L.: Oscillation and chaos in physiological control systems. *Science* **197**, 287–289 (1977)
15. Hornykiewicz, O., Kish, S.J.: Biochemical pathophysiology of Parkinson's disease. *Adv. Neurol.* **45**, 19–34 (1987)
16. Alexander, G.E., Crutcher, M.D., DeLong, M.R.: Basal ganglia-thalamocortical circuits: parallel substrates for motor, oculomotor, "prefrontal" and "limbic" functions. *Prog. Brain Res.* **85**, 119–146 (1990)
17. Plenz, D., Kitai, S.T.: A basal ganglia pacemaker formed by the subthalamic nucleus and external globus pallidus. *Nature* **400**, 677–682 (1999)
18. Terman, D., Rubin, J.E., Yew, A.C., Wilson, C.J.: Activity patterns in a model for the subthalamo-pallidal complex of the basal ganglia. *J. Neurosci.* **22**, 2963–2976 (2002)
19. Gillies, A., Willshaw, D.: Models of the subthalamic nucleus: the importance of intranuclear connectivity. *Med. Eng. Phys.* **26**, 723–732 (2004)
20. Rubin, J.E., Terman, D.: High frequency stimulation of the subthalamic nucleus eliminates pathological thalamic rhythmicity in a computational model. *J. Comput. Neurosci.* **16**, 211–235 (2004)
21. Titcombe, M., Glass, L., Guehl, D., Beuter, A.: Dynamics of tremor during deep brain stimulation. *Chaos* **11**, 766–773 (2001)
22. Beuter, A., Titcombe, M.S., Richer, F., Gross, C., Guehl, D.: Effect of deep brain stimulation on amplitude and frequency characteristics of rest tremor in Parkinson's disease. *Thalamus Relat. Syst.* **1**, 203–211 (2001)
23. Levy, R., Hutchison, W.D., Lozano, A.M., Dostrovsky, J.O. High-frequency synchronization of neuronal activity in the subthalamic nucleus of Parkinsonian patients with limb tremor. *J. Neurosci.* **20**, 7766–7775 (2000)
24. Foffani, G., Ardolino, G., Egidio, M., Caputo, E., Bossi, B., Priori, A.: Subthalamic oscillatory activities at beta or higher frequency do not change after high-frequency DBS in Parkinson's disease. *Brain Res. Bull.* **69**, 123–130 (2006)
25. Wilson, H.R., Cowan, J.D.: A mathematical theory of the functional dynamics of cortical and thalamic nervous tissue. *Kybernetik* **13**, 55–80 (1973)
26. Dayan, P., Abbott, L.F.: *Theoretical Neuroscience: Computational and Mathematical Modeling of Neural Systems*. MIT, Cambridge (2001)
27. Izhikevich, E.M.: *Dynamical Systems in Neuroscience*. MIT, Cambridge (2007)
28. Izhikevich, E.M.: Simple model of spiking neurons. *IEEE Trans. Neural Netw.* **14**, 1569–1572 (2003)
29. Modolo, J., Mosekilde, E., Beuter, A.: New insights offered by a computational model of deep brain stimulation. *J. Physiol. Paris* **101**, 58–65 (2007)
30. Modolo, J., Garenne, A., Henry, J., Beuter, A.: Development and validation of a population density based model of Izhikevich neurons. *J. Integr. Neurosci.* **6**, 625–655 (2007)
31. Levesque, J.C., Parent, A.: GABAergic interneurons in human subthalamic nucleus. *Mov. Disord.* **20**(5), 574–584 (2005)
32. Nykamp, D.Q., Tranchina, D.: A population density approach that facilitates large-scale modeling of neural networks: analysis and an application to orientation tuning. *J. Comput. Neurosci.* **8**, 19–50 (2000)
33. Bevan, M.D., Wilson, C.J.: Mechanisms underlying spontaneous oscillation and rhythmic firing in rat subthalamic neurons. *J. Neurosci.* **19**, 7617–7628 (1999)

34. Garcia, L., Audin, J., D'Alessandro, G., Bioulac, B., Hammond, C.: Dual effect of high-frequency stimulation on subthalamic neuron activity. *J. Neurosci.* **23**, 8743–8751 (2003)
35. Timmermann, L., Wojtecki, L., Gross, J., Lehrke, R., Voges, J., Maarouf, M., Treuer, H., Sturm, V., Schnitzler, A.: Ten-Hertz stimulation of subthalamic nucleus deteriorates motor symptoms in Parkinson's disease. *Mov. Disord.* **19**, 1328–1333 (2004)
36. Fogelson, N., Kuhn A.A., Silberstein, P., Limousin, P.D., Hariz, M., Trottenberg, T., Kupsch, A., Brown, P.: Frequency dependent effects of subthalamic nucleus stimulation in Parkinson's disease. *Neurosci. Lett.* **382**, 5–9 (2005)
37. Albin, R., Young, A., Penney, J.: The functional anatomy of basal ganglia disorders. *Trends Neurosci.* **12**, 366–375 (1989)
38. Merrill, D.R., Bikson, M., Jefferys, J.G.R.: Electrical stimulation of excitable tissue: design of efficacious and safe protocols. *J. Neurosci. Meth.* **141**(2), 171–198 (2005)
39. Boraud, T., Brown, P., Goldberg, J.A., Graybiel, A.M., Magill, P.J.: Oscillations in the basal ganglia: the good, the bad and the unexpected. In: Bolam, J.P., Ingham, C.A., Magill, P.J. (eds.) *The Basal Ganglia VIII*. Springer Science and Business Media, New York (2005)
40. Burbaud, P., Gross, C., Bioulac, B.: Effect of subthalamic high frequency stimulation on substantia nigra pars reticulata and globus pallidus neurons in normal rats. *J. Physiol. Paris* **88**, 359–361 (1994)
41. Beuter, A., Modolo, J., Edwards, R.: Differential effect of DBS stimulation of GPi and STN on Parkinsonian tremor. IBAGS Conference, Amsterdam (2007)
42. Cilia, R., Marotta, G., Landi, A., Isaias, I.U., Vergani, F., Benti, R., Sganzerla, E., Gerundini, P., Pezzoli, G., Antonini, A.: Cerebral activity modulation by extradural motor cortex stimulation in Parkinson's disease: a perfusion SPECT study. *Eur. J. Neurol.* **15**(1), 22–28 (2008)